G Model
ETP50748 1–11
ARTICLE IN PRESS

Experimental and Toxicologic Pathology xxx (2012) xxx–xxx

Contents lists available at SciVerse ScienceDirect

Experimental and Toxicologic Pathology

journal homepage: www.elsevier.de/etp

Thickened area of external granular layer and Ki-67 positive focus are early events of medulloblastoma in *Ptch1*$^{+/-}$ mice

Q1 Saori Matsuo[a,d], Miwa Takahashi[a], Kaoru Inoue[a], Kei Tamura[a], Kaoru Irie[a], Yukio Kodama[b], Akiyoshi Nishikawa[c], Midori Yoshida[a,*]

[a] Division of Pathology, National Institute of Health Sciences, 1-18-1 Kamiyoga, Setagaya-ku, Tokyo 158-8501, Japan
[b] Division of Toxicology, National Institute of Health Sciences, 1-18-1 Kamiyoga, Setagaya-ku, Tokyo 158-8501, Japan
[c] Biological Safety Research Center, National Institute of Health Sciences, 1-18-1 Kamiyoga, Setagaya-ku, Tokyo 158-8501, Japan
[d] Pathogenetic Veterinary Science, United Graduate School of Veterinary Sciences, Gifu University, 1-1 Yanagido, Gifu-shi, Gifu 501-1193, Japan

ARTICLE INFO

Article history:
Received 3 September 2012
Received in revised form
26 November 2012
Accepted 14 December 2012

Keywords:
Cerebellar development
Granule cell precursors
Medulloblastoma
Patched1
Preneoplastic lesion
Sonic hedgehog

ABSTRACT

Patched1 (Ptch1) encodes a receptor for Sonic hedgehog (Shh) and is major gene related to human medulloblastoma (MB) in the Shh subgroup. MB is thought to arise from residual granule cell precursors (GCPs) located in the external granular layer (EGL) of the developing cerebellum. As the detailed preneoplastic changes of MB remain obscure, we immunohistochemically clarified the derived cell, early events of MBs, and the cerebellar developmental processes of *Ptch1*$^{+/-}$ (Ptch1) mice, an animal model of human MB of the Shh subgroup. In Ptch1 mice, the earliest proliferative lesions were detected at PND10 as focal thickened areas of outer layer of the EGL. This area was composed of GCP-like cells with atypia and nuclei disarrangement. In the latter cerebellar developmental period, GCP-like cell foci were detected at high incidence in the outermost area of the cerebellum. Their localization and morphological similarities indicated that the foci were derived from GCPs in the EGL. There were two types of the foci. A Ki-67-positive focus was found in Ptch1 mice only. This type resembled the GCPs in the outer layer of EGL characterized by having proliferating activity and a lack of neuronal differentiation. Another type of focus, Ki-67-negative, was observed in both genotypes and exhibited many of the same features of mature internal granule cells, suggesting that the focus had no preneoplastic potential. Due to morphological, immunohistochemical characteristics, our results indicate that the focal thickened area of EGL and Ki-67-positive foci are preneoplastic lesions of MB.

1. Introduction

Medulloblastoma (MB) is the most common malignant tumor in children which shows tremendous biological and clinical heterogeneity (Dhall, 2009; Hatten and Roussel, 2011; Jones et al., 2012). Q2 MB in humans is classified into four subtypes with distinct clinical, biological, and genetic profiles (Aref et al., 2012; Ellison et al., 2011; Jones et al., 2012; Kool et al., 2012; Mohan et al., 2012; Northcott et al., 2011). Molecular analysis of Sonic hedgehog (Shh) tumors in humans revealed activation of the Shh signaling pathway due to the loss of *Patched1 (Ptch1)* and mutations in other components of the Shh pathway. Approximately as high as 30% of MBs have mutations in Shh pathway components (Bhatia et al., 2012; Crawford et al., 2007; Klesse and Bowers, 2010; Oliver et al., 2005; Roussel and Hatten, 2011; Wang et al., 2012). *Ptch1* encodes a receptor for Shh, Patched1 (Ptch1), and is one of the major genes related to MB formation in humans (Dhall, 2009; Raffel, 2004). A subset of MBs has been identified with allelic loss of chromosome 9q22, a region that contains *Ptch1* (Dhall, 2009; Raffel, 2004). Pathway activation is triggered by binding of Shh to Ptch1, which in the absence of Shh suppresses the activity of Smoothened (Smo). Shh binding to Ptch1 or mutational inactivation of Ptch1 relieves the inhibition of Smo culminating in the activation of one or more of the Gli1 transcription factors that regulate the expression of downstream targets (Huse and Holland, 2010; Roussel and Hatten, 2011). Inappropriate activation of the Shh pathway is accepted as a cause of familial cancer due to inherited mutation of the *Ptch1* gene, which has been identified as responsible for nevoid basal cell carcinoma syndrome (Dhall, 2009; Klesse and Bowers, 2010).

Heterozygous *Ptch1* knockout mice (Ptch1 mice) display many of the typical symptoms of nevoid basal cell carcinoma syndrome, also known as Gorlin syndrome, including skeletal abnormalities, neural tube closure defects, a generalized over-growth, and predisposition to tumor formation (Corcoran and Scott, 2001; Hahn et al., 1999; Raffel, 2004). In addition, the Ptch1 mouse strain displays a high yield (14% up to 30%) of MB that resembles human

* Corresponding author. Tel.: +81 3 3700 9821; fax: +81 3 3700 1425.
E-mail address: modoriy@nihs.go.jp (M. Yoshida).

0940-2993/$ – see front matter © 2012 Published by Elsevier GmbH.
http://dx.doi.org/10.1016/j.etp.2012.12.005

Please cite this article in press as: Matsuo S, et al. Thickened area of external granular layer and Ki-67 positive focus are early events of medulloblastoma in *Ptch1*$^{+/-}$ mice. Exp Toxicol Pathol (2012), http://dx.doi.org/10.1016/j.etp.2012.12.005

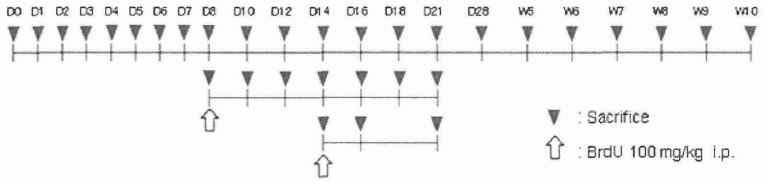

Fig. 1. Experimental design. Schedules for necropsy and the administration of BrdU are illustrated. Each time point represents at least 2 wild-type mice and 6 Ptch1 mice from over 2 dams. D, postnatal day; W, postnatal week.

MB of the Shh subgroup (Goodrich et al., 1997; Lau et al., 2012; Wetmore et al., 2000). In the mice, homozygous loss of *Ptch1* results in embryonic lethality at 9.5–10.5 days after fertilization (Goodrich et al., 1997). Thus, heterozygous *Ptch1* knockout mice have been used as a model for nevoid basal cell carcinoma/Gorlin syndrome including human MB, rhabdomyosarcoma, and basal cell carcinoma (Corcoran and Scott, 2001; Dyer, 2004; Hahn et al., 1999; Pazzaglia, 2006; Wu et al., 2011). Although Ptch1 mice are a valuable model for evaluation of drug efficacy and modulating effects of additional gene mutations, chemicals, or irradiation on brain tumor formation in childhood, the long latent period of 9 to over 12 months for assessment results in clinical signs of increased intracranial pressure (ataxia, decreased movement, paresis of hind limbs, enlarged occipital prominence, hunched back, and/or poor grooming) and death (Ayrault et al., 2009; Briggs et al., 2008; Ecke et al., 2009; Farioli-Vecchioli et al., 2007; Kimura et al., 2005; Pazzaglia et al., 2006, 2009; Pogoriler et al., 2006; Takahashi et al., 2012; Uziel et al., 2005; Wetmore et al., 2001). Therefore, detection of early indicators of MBs such as preneoplastic lesions in Ptch1 mice and evaluation with changes as an indicator of MB in short-term studies is needed.

To find early indicators of tumors in childhood, detailed investigation of normal developmental processes of target organs can be useful. Human MBs are thought to be derived from residual granule cell precursors (GCPs) located in the external granule cell or external granular (germinal) layer (EGL) of the cerebellum, although GCPs migrate inward to form the internal granule cell or internal granular layer (IGL) during normal cerebellar development (Behesti and Marino, 2009; Haldipur et al., 2012; Roussel and Hatten, 2011). The processes of cerebellar and MB development in Ptch1 mice are not well-defined.

This study was conducted to clarify the derived cell and early events of MBs, and cerebellar developmental processes in Ptch1 mice. We examined cerebella of Ptch1 mice and wild-type littermates sequentially during postnatal day (PND) 0 to 10 weeks of age.

2. Materials and methods

2.1. Animals

Ptch1 heterozygous knockout mice, generated by replacing exon 1 and 2 of the ptch1 gene with a LacZ/neomycin cassette (Goodrich et al., 1997), were obtained from The Jackson Laboratory (Bar Harbor, ME, USA) and maintained in our laboratory. They were housed in polycarbonate cages with wood chip bedding and maintained in an air-conditioned animal room (temperature 24 ± 1 °C, relative humidity 55 ± 5%, 12-h light–dark cycle) with basal diet (CRF-1, Oriental Yeast Co., Tokyo, Japan) and tap water available *ad libitum*. The experimental protocol using animals was reviewed and approved by the Animal Care and Use Committee of the National Institute of Health Sciences, Japan.

2.2. Necropsy

To examine following morphologic analysis necropsy was performed according to protocol (Fig. 1). Ptch1 and wild-type littermate mice were euthanized under deep anesthesia with isoflurane. 2–11 wild-type mice and 6–19 Ptch1 mice were analyzed at each time point from at least two litters.

2.3. Genotyping

Animals were genotyped by PCR amplification of genomic DNA extracted from the tail. The wild type allele was distinguished with primers 5′-CTG CGG CAA GTT TTT GGT TG-3′ and 5′-AGG GCT TCT CGT TGG CTA CAA C-3′, which yield a 200-bp PCR product. The mutant allele was detected using primers 5′-GCC CTG AAT GAA CTG CAG GAC G-3′ and 5′-CAC GGG TAG CCA ACG CTA TGT C-3′, which yield a 479-bp PCR product.

2.4. BrdU labeling

To examine migration of GCPs, a single intraperitoneal injection of 100 mg/kg body weight of 5-Bromo-2′-deoxyuridine (BrdU, CAS No. 59-14-3 Sigma–Aldrich, MO, USA) in saline (Otsuka Pharmaceutical Factory, Inc., Japan) was given to mice at PND8 and 14. Animals treated with BrdU at PND8 were euthanized as above 1.5 h after the injection and at PND10, 12, 14, 16, 18, and 21. Animals treated with BrdU at PND14 were euthanized 1.5 h after injection and at PND16 and 21 (Fig. 1).

Table 1
Primary antibodies used for immunohistochemistry.

Antigen	Clone	Concentration/dilution	Antigen retrieval	Visualization system	Source
BrdU	BU1/75(ICR1)	1 μg/mL	Autoclave	LSAB	AbD serotec
Ki-67	TEC-3	30 μg/mL	Autoclave	LSAB	Dako
NeuN	A60	3 μg/mL	Autoclave	Polymer	Millipore
$p27^{kip1}$	EP233(2)Y	1:2000	Autoclave	Polymer	Abcam
Nestin	Rat-401	3 μg/mL	Autoclave	Polymer	Millipore
CyclinD1	EPR2241(IHC)-32	1:300	Autoclave	Polymer	Millipore
GFAP	Polyclonal	1 μg/mL	Microwave	Polymer	Dako
Calbindin-D-28K	CB-955	3 μg/mL	Microwave	Polymer	Sigma–Aldrich

Please cite this article in press as: Matsuo S, et al. Thickened area of external granular layer and Ki-67 positive focus are early events of medulloblastoma in *Ptch1*$^{+/-}$ mice. Exp Toxicol Pathol (2012), http://dx.doi.org/10.1016/j.etp.2012.12.005

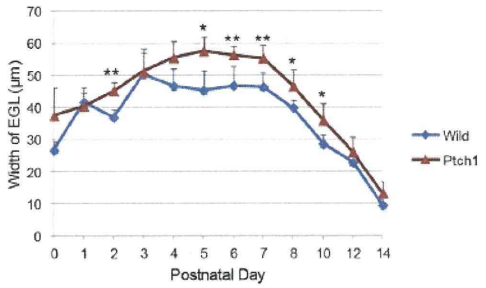

Fig. 2. Changes in the width of EGL in developing cerebellum of Ptch1 and wild-type mice from PND0 to PND10. *, **: Significantly different from wild-type mice at $P < 0.05$ and $P < 0.01$, respectively.

2.5. Tissue processing

After detailed necropsy, brains were removed and fixed in 10% neutral buffered formalin. Midsagittal sections of cerebella were routinely processed for paraffin embedding, sectioned and stained with hematoxylin and eosin. The prepared histopathological specimens were examined under light microscopy.

2.6. Morphometric assessment

Photomicrographs of midsagittal sections of the cerebellum were taken with a digital camera attached to microscope (DP71, Olympus Corp., Tokyo, Japan), and then measurement was performed using image analysis software (WinROOF, Version 5.7.1, Mitani Corp., Tokyo, Japan). The numbers of wild-type and Ptch1 mice measured at each time point were 3–6 obtained from 2 to 5 litters (mainly 3–5 litters) except for Ptch1 mice at PND10. At PND10, five mice were obtained from the same dam. The width of the EGL of each mouse was determined by five measurements selected at random from the entire cerebellum (PND0 to 2) or 4th/5th cerebellar lobules (PND3 to 14).

2.7. Immunohistochemistry

Antibodies used for immunohistochemistry included monoclonal rat anti-BrdU (AbD serotec, Oxford, UK), monoclonal rat anti-mouse Ki-67 (Dako Cytomation, Glostrup, Denmark) as proliferation marker, monoclonal mouse anti-NeuN (Millipore, MA, USA) as a mature granule cell marker, monoclonal rabbit anti-$p27^{kip1}$ (Abcam, Tokyo, Japan) as a postmitotic granule cell marker, monoclonal mouse anti-Nestin (Millipore) as a neuronal stem cell marker, monoclonal rabbit anti-CyclinD1 (Millipore) as a proliferating GCPs marker, polyclonal rabbit anti-GFAP (Dako Cytomation) as a Bergmann glia marker, and monoclonal mouse

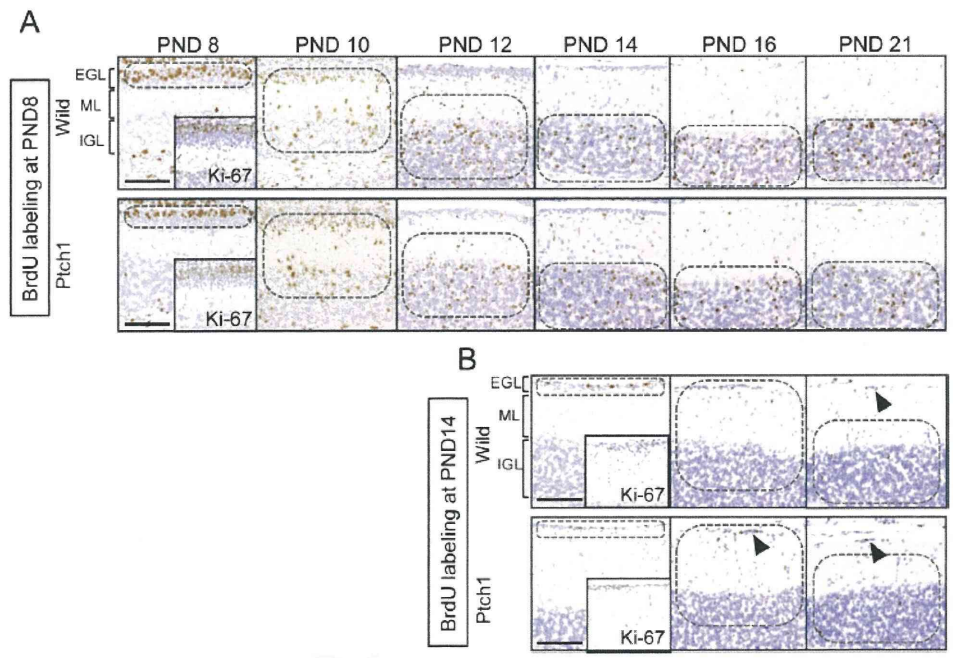

Fig. 3. Migration of GCPs of wild-type and Ptch1 mice from PND8 to PND21. (A) Sequential migration of GCPs labeled with BrdU at PND8 (1.5 h after injection) of wild-type (top row) and Ptch1 mice (bottom row). BrdU-positive cells were observed in Ki-67-positive, proliferating outer layers of the EGL 1.5 h later (PND8). At PND10 (2 days after injection), most of the BrdU-positive cells were localized in the inner layer of the EGL, molecular layer (ML), and IGL. The EGL almost disappeared at PND16 and most of the BrdU-positive cells finished migrating into the IGL by PND21. (B) Sequential migration of GCPs labeled with BrdU at PND14 of wild-type (top row) and Ptch1 mice (bottom row). BrdU-positive cells were observed in 1–3 layers of Ki-67-positive, proliferating cells of the EGL at PND14 (1.5 h after injection). From PND16 onwards when most of GCPs finished migrating from the EGL, small foci with GCP-like cells labeled with BrdU were detected in the outermost regions of cerebellar cortex (arrowhead). Circle indicates major location of BrdU-labeled GCPs. Scale bar: 100 μm.

Please cite this article in press as: Matsuo S, et al. Thickened area of external granular layer and Ki-67 positive focus are early events of medulloblastoma in *Ptch1*$^{+/-}$ mice. Exp Toxicol Pathol (2012), http://dx.doi.org/10.1016/j.etp.2012.12.005

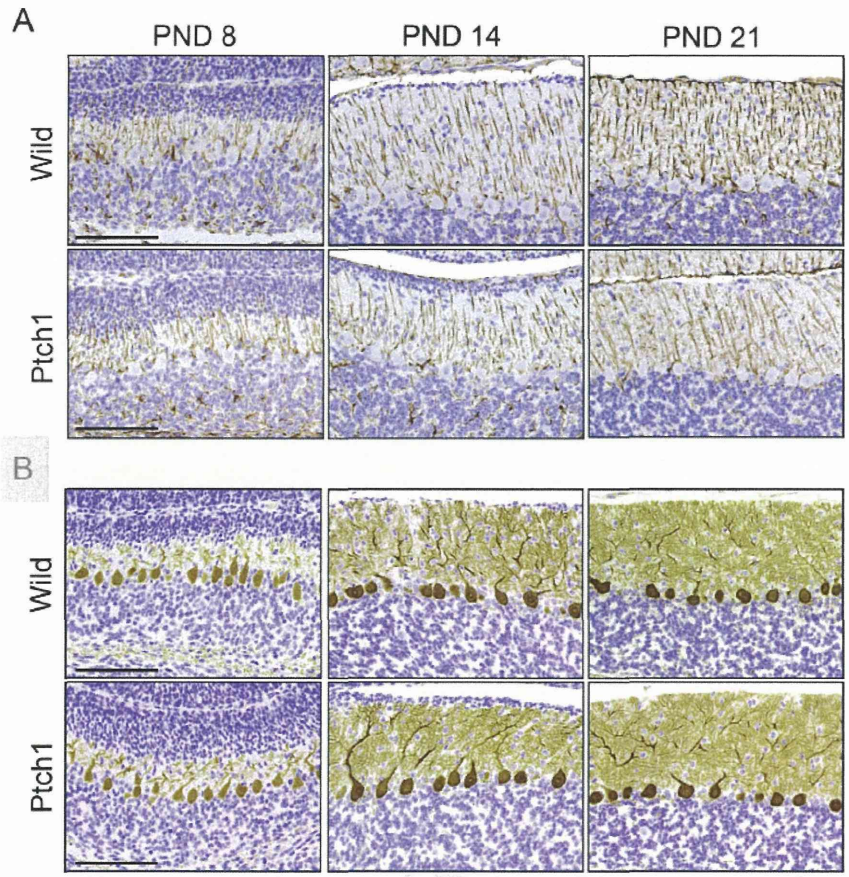

Fig. 4. Bergmann glia and Purkinje cells in the developing cerebellum of wild-type and Ptch1 mice. (A) Bergmann glia of wild-type (top row) and Ptch1 mice (bottom row) stained with anti-GFAP antibody at PND8, 14, and 21. No morphological abnormalities were observed in Ptch1 mice compared to wild-type mice. (B) Purkinje cells of wild-type (top row) and Ptch1 mice (bottom row) stained with anti-Calbindin-D-28K antibody at PND8, 14, and 21. No morphological abnormalities were observed in Ptch1 mice compared to wild-type mice. Scale bars: 100 μm.

anti-Calbindin-D-28K (Sigma–Aldrich, MO, USA) as a Purkinje cell marker. A labeled streptavidin-biotin method was applied for anti-BrdU and Ki-67 antibodies using polyclonal rabbit anti-rat biotinylated IgG (Dako Cytomation) and streptavidin-conjugated horseradish peroxidase (Dako Cytomation). A polymer method was applied for the rest of the primary antibodies using Histofine Simple Stain kit (Nichirei Biosciences Inc., Tokyo, Japan). The immunoreactions were visualized by peroxidase-diaminobenzidine reaction. The sections were then counterstained lightly with hematoxylin. Table 1 provides details of protocols for the immunohistochemistry and information of the antibodies.

2.8. Statistical analysis

The width of the EGL was analyzed by Student's *t*-test following a test for equal variance.

3. Results

3.1. General remarks

There were no significant differences in body weight from PND0 to PND21 among the genotypes of intact animals (data not shown). Mortality and body weight of mice were not affected by injection of BrdU. No clinical signs were detected in wild-type and Ptch1 mice. At necropsy, swelling of cerebellum and obscurity of lobular structure with a lack of cerebellar foliation which were diagnosed as MB microscopically were observed in Ptch1 mice at PND28 and W5. Hydrocephalus showing slight dilatation of ventricles of cerebrum and masses of skeletal muscles near the ribs or sternums and in the abdominal muscles were noted after PND3 in Ptch1 mice only. These intramuscular masses were diagnosed microscopically as rhabdomyosarcomas. Macroscopically, there was no

Please cite this article in press as: Matsuo S, et al. Thickened area of external granular layer and Ki-67 positive focus are early events of medulloblastoma in *Ptch1*$^{+/-}$ mice. Exp Toxicol Pathol (2012), http://dx.doi.org/10.1016/j.etp.2012.12.005

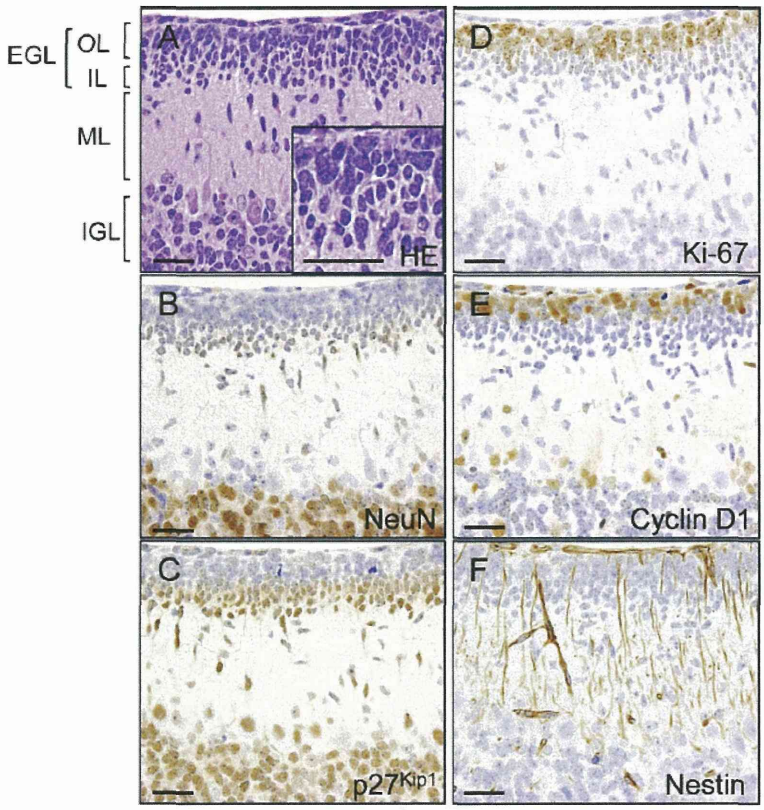

Fig. 5. Morphology and immunohistochemistry of the developing cerebellum. Representative morphology and immunohistochemistry of the developing cerebellar cortex from Ptch1 mice (PND10). Their characteristics were common to both genotypes. (A) HE staining of the cerebellar cortex. EGL with asterisk was magnified (inset). (B) NeuN was weakly positive in the inner layer of the EGL (IL) and migrating granular cells in the molecular layer (ML) and strongly positive in the IGL. (C) $p27^{kip1}$ was strongly positive in the IL and migrating granular cells in the ML and positive in the IGL. (D) Granular cells in the outer layer of the EGL (OL) were positive for Ki-67. (E) Granular cells in the OL were positive for Cyclin D1. (F) Positive staining for Nestin was observed radically from the surface of the cerebellum to the IGL in a straight line. Scale bars: 25 μm.

metastatic lesion of MB and rhabdomyosarbomas in tumor-bearing mice.

3.2. Sequential changes in the width and migration process of the EGL

Postnatal changes in the width of the EGL in wild-type and Ptch1 mice are shown in Fig. 2. The width of the EGL peaked at PND5 to 7 and the width in Ptch1 mice was greater than in wild-type mice during PND5 to 10.

Fig. 3 shows localization of BrdU-positive cells injected in mice at PND8 (Fig. 3A) and PND14 (Fig. 3B), respectively. GCPs in the outer layer of the EGL were the only cell type to be positive for BrdU in the EGL. In animals injected with BrdU at PND8, BrdU-positive cells were observed in the outer layer of the EGL which was positive for Ki-67 1.5 h after the injection (Fig. 3A and A insets). BrdU-positive EGL cells gradually migrated into the IGL accompanied by thinning of the EGL in both genotypes. At PND16, only one layer of the EGL was present and then disappeared at PND21 in both genotypes.

3.3. Sequential changes of Purkinje cells and Bergmann glia in the developing cerebellum

Purkinje cells and Bergmann glia are major components of the cerebellum and have important roles in cerebellar development. Long processes of the radial glial cells, Bergmann glia, were visualized by immunohistochemistry with anti-GFAP antibody (Fig. 4A). For both genotypes, there was no difference in the density or extending direction of the processes at PND0 to 21. In addition, Purkinje neurons (including dendritic arbors) were stained with anti-Calbindin-D-28K antibody. From qualitative microscopic inspection a difference in the number, alignment, or arborization of Purkinje cells was not detected between the genotypes during postnatal cerebellar development.

3.4. Morphology and immunohistochemical characteristics of granule cells in the developing cerebellum

Morphology and immunohistochemical reactions to antibodies related to cell proliferation and neuronal differentiation revealed

Please cite this article in press as: Matsuo S, et al. Thickened area of external granular layer and Ki-67 positive focus are early events of medulloblastoma in *Ptch1*$^{+/-}$ mice. Exp Toxicol Pathol (2012), http://dx.doi.org/10.1016/j.etp.2012.12.005

Table 2
Morphological characteristic of granular precursor cells located in EGL, molecular layer, and IGL in developing cerebellum at PND0 to 14.

	EGL		Molecular layer	IGL
	Outer layer	Inner layer		
Histopathology				
	Medium–large size Round–polygonal	Small size Oval–elongate (vertical)	Small size Oval–spindle (vertical)	Medium size Round
Immunohistochemistry				
Ki-67	+	–	–	–
CyclinD1	+	–	–	–
NeuN	–	±	±	+/++
$p27^{kip1}$	–	++	+/++	+
Nestin	+	+	+	±[a]/–[b]

–, negative; ±, weakly positive; +, positive; ++, strongly positive. These characteristics shown in the table are common to all time points measured (PND0 to 14); except for Nestin staining in the IGL.
[a] Until PND10.
[b] Day after PND10.

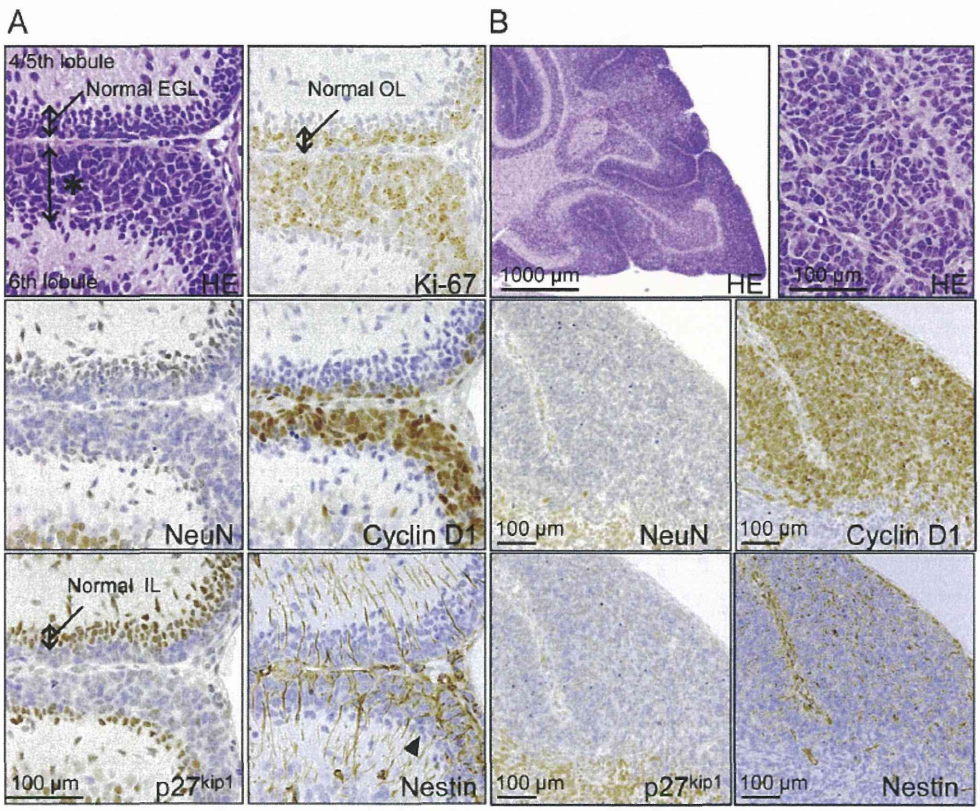

Fig. 6. Proliferative lesions in the developing cerebellum in Ptch1 mice at PND10 and 12. (A) A thickened proliferative lesion (asterisk) in the outer layer of the EGL (6th lobule) in Ptch1 mice at PND10. The 4th/5th lobule showed normal EGL structure. In this lesion, the outer layer of the EGL stained with Ki-67 and cyclinD1 was expanded. The inner layer of the EGL (IL) stained with NeuN and $p27^{kip1}$ was thinned compared to the normal IL in the 4th/5th lobule. Positive staining for Nestin was observed intracellularly in all directions in this lesion (arrowhead). Scale bar: 100 μm. (B) MB in Ptch1 mice at PND12. Higher magnification of HE staining showed that proliferating cells resembled thickened lesions of the outer layer of the EGL.

Please cite this article in press as: Matsuo S, et al. Thickened area of external granular layer and Ki-67 positive focus are early events of medulloblastoma in *Ptch1*$^{+/-}$ mice. Exp Toxicol Pathol (2012), http://dx.doi.org/10.1016/j.etp.2012.12.005

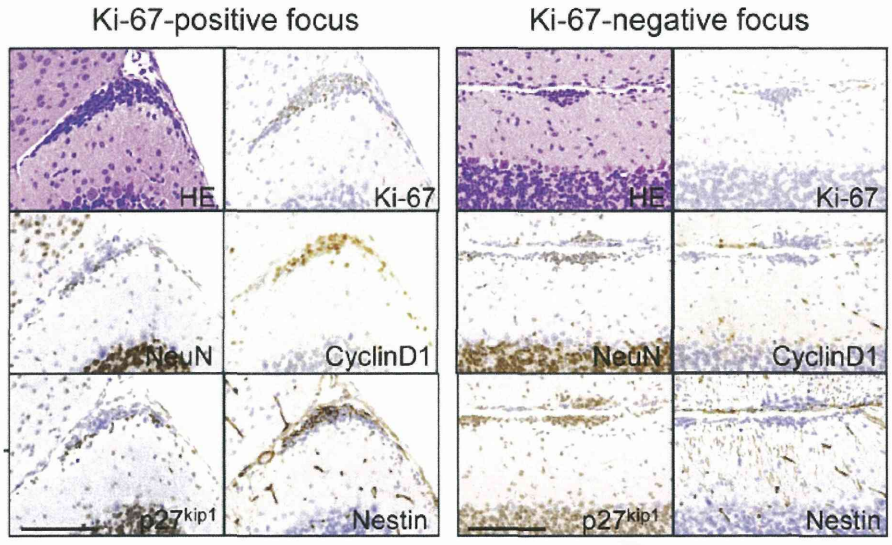

Fig. 7. Immunohistochemical characterization of foci composed of GCP-like cells. Ki-67-positive (left) and Ki-67-negative (right) foci of Ptch1 mice. Ki-67-positive foci were composed of medium to large-sized, round to polygonal nuclei that were negative or weakly positive for NeuN and $p27^{kip1}$ and positive for cyclin D1 and nestin, indicating unclear differentiation into neuronal cells. Ki-67-negative foci were composed of round and small nuclei that were positive for NeuN and $p27^{kip1}$ and negative for Cyclin D1 and nestin, indicating differentiation into neural cells similar to IGL cells. Scale bar: 50 μm.

that the structure of the developing cerebellum was common to both genotypes (Table 2 and Fig. 5). Nuclei of GCPs in the outer layer of the EGL were medium to large-sized and round to polygonal. These cells were positive for Ki-67 and Cyclin D1 and negative for NeuN and $p27^{kip1}$. Inner layer EGL nuclei were small-sized, oval to elongate, and arranged vertically. In this layer, granular cells were negative for Ki-67 and Cyclin D1, weakly positive for NeuN and strongly positive for $p27^{kip1}$. Migrating granular cells in the molecular layer were oval to spindle shaped small cells arranged vertically and had the same staining profiles as inner layer EGL nuclei. Granular cells with medium-sized round nuclei in the IGL surrounded eosinophilic mossy fibers. Those were negative for Ki-67 and Cyclin D1 and positive to strongly positive for NeuN and $p27^{kip1}$. Positive staining for nestin was observed radically throughout the cerebellar cortex, and weak staining in the IGL remained until PND10.

3.5. Changes in the developing cerebellum and derived cells

Proliferative lesions were observed in the developing cerebellum in Ptch1 mice. Proliferation of GCP-like cells was observed in a thickened area of the EGL, which was continuous from the normal EGL on and after PND10 in Ptch1 mice (Fig. 6A, asterisk). The proliferative lesions substituted for the inner layer of the EGL (Fig. 6A). Moreover, early occurrence of MB was detected at PND12 (Fig. 6B). In both proliferative lesions, large-sized, round to polygonal cells with atypia were main components. Immunohistochemically, the cells were positive for Cyclin D1 and nestin and weakly positive or negative for NeuN and $p27^{kip1}$. Intercellular irregular nestin staining was distinctive of these lesions (Fig. 6A arrowhead and B), as nestin-positive fibers were arranged regularly and radically in a straight line in the normal EGL (Figs. 5F and 6A). Histopathology and immunohistochemistry of these proliferative lesions resembled GCPs in the outer layer of the EGL of the normal cerebellum.

After PND16, the time when migration of EGL cells to the IGL has almost completed, foci with GCP-like cells were detected in the outermost region of the cerebellar cortex in the cerebella of mice from both genotypes (Figs. 3B and 7). In the mice injected with BrdU at PND14, BrdU-positive cells were detected in the EGL 1.5 h after treatment (Fig. 3B) and BrdU-positive cells had migrated into the deep molecular layer and the IGL by PND21 (Fig. 3). As some of the GCP-like cells of the foci in mice injected with BrdU at PND14 were positive for BrdU after PND16, the cells were considered to be derived from the residual GCPs in the EGL (Fig. 3B, arrowhead). The residual foci were clearly classified into two types: Ki-67-positive and Ki-67-negative (Fig. 7). Ki-67-positive foci were composed of atypical cells whose nuclei were medium to large-sized and round to polygonal in shape (Fig. 7, left). The cells were immunohistochemically negative or weakly positive for NeuN and $p27^{kip1}$ and positive for cyclin D1 and nestin (Fig. 7, left). Conversely, Ki-67-negative foci were composed of cells with round and small shaped nuclei. The cells were positive for NeuN and $p27^{kip1}$ and negative for nestin and cyclin D1, indicating differentiation into neural cells (Fig. 7, right). Some of Ki-67-negative foci contained a strongly eosinophilic area resembling mossy fibers among the nuclei (Fig. 8, asterisk) and they were comparable to the structure of the IGL.

3.6. Relationship between residual foci of GCPs and MBs

The incidences of Ki-67-positive or negative foci and MBs were investigated from PND16 up to 10 weeks of age in both genotypes (Fig. 9). MBs were divided into two types: a focal MB occupying one to two lobules of the cerebellum was defined as a small MB and an advanced MB spreading over three or more lobules was defined as a large MB. In Ptch1 mice, Ki-67-positive foci, small MB, and large MB were observed and most of the mice had Ki-67-negative foci. The peak of Ki-67-positive foci was up to PND21, the completion period of cerebellar development. The incidences of MBs were comparable

Please cite this article in press as: Matsuo S, et al. Thickened area of external granular layer and Ki-67 positive focus are early events of medulloblastoma in *Ptch1*$^{+/-}$ mice. Exp Toxicol Pathol (2012), http://dx.doi.org/10.1016/j.etp.2012.12.005

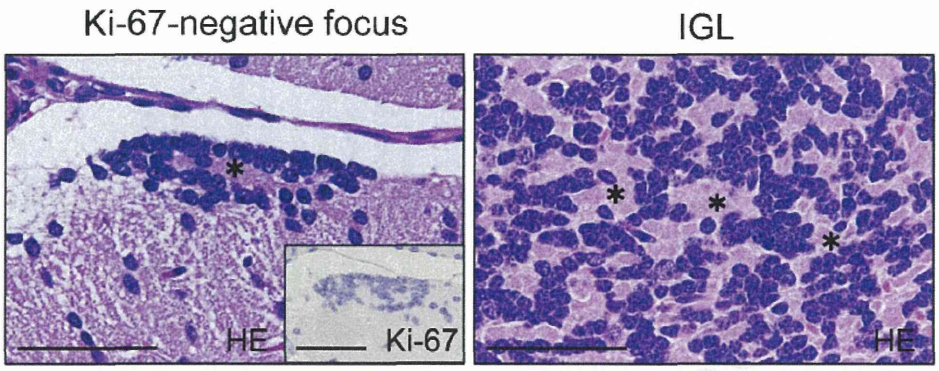

Fig. 8. Ki-67-negative foci showing differentiation into the IGL. HE staining of Ki-67-negative focus (left) and the IGL (right) of Ptch1 mice at PND21. An eosinophilic mossy fiber-like substance (arrowhead) was surrounded by nuclei of Ki-67-negative focus. Mossy fibers (asterisk) were observed among the nuclei of granular cells of the IGL. Scale bar: 50 μm.

between ages. In wild-type mice, no proliferative lesions, neither Ki-67-positive foci nor MBs other than Ki-67-negative foci, were detected at any age (Fig. 9). The incidence of Ki-67-negative foci decreased with increased age in wild-type mice. The number of Ki-67-negative foci per animal was larger in Ptch1 mice as compared to wild-type mice (data not shown).

Examination for localization of each change revealed that more than 70% of Ki-67-negative foci were localized in the 6–10th lobules of the cerebellum in both genotypes (Fig. 10). In addition, more than 50% of Ki-67-positive foci and small MBs were also observed in the 6–10th lobules in Ptch1 mice (Fig. 10).

4. Discussion

The present study was performed to clarify derived cell and early changes of MBs in Ptch1 mice using immunohistochemistry. We also compared cerebellar developmental processes in Ptch1 mice to wild-type mice. Currently, human MBs are classified as four distinct subtypes by molecular studies (Ellison et al., 2011; Northcott et al., 2011; Jones et al., 2012; Kool et al., 2012). Tumors of Ptch1 mice are thought to be equivalent for those of the Shh subgroup in human (Lau et al., 2012). Therefore, MBs in Ptch1 mice will be good tool for testing new drugs targeting the Shh pathway. Additionally, detailed investigation of the cerebellar development and early changes of MB in Ptch1 mice will be beneficial to understanding pathogenesis of human MBs.

During the experimental period, Ptch1 mice showed no clinical signs except development of hydrocephalus and rhabdomyosarcomas in some cases, an outcome that has been previously described (Corcoran and Scott, 2001; Wetmore et al., 2000; Svärd et al., 2009). Although the pathogenesis of hydrocephalus in Ptch1 mice has not been fully understood, impaired cilia function of the ependymal cells might be related (Gavino and Richard, 2011).

The present study demonstrated that a single injection of BrdU was useful in pursuing the sequential migrating process of GCPs from the EGL to the IGL. Similar to results of another study (Thomas et al., 2009), we observed that the migration process in Ptch1 mice was the same as that in wild-type mice and that the proliferation of GCPs increased in Ptch1 mice resulting in a slightly wider EGL layer. No clear evidence was obtained, but the increased proliferation in the EGL in Ptch1 mice might be related to the high potential for MB described below. Shh signaling regulates the expansion of the pool of GCPs (Roussel and Hatten, 2011; Wang et al., 2012). Reduced levels of Ptch1 expression in the cerebellum of Ptch1 mice might be caused by loss of one allele resulting in increased proliferation of GCPs (Corcoran and Scott, 2001; Goodrich et al., 1997; Gupta et al., 2010; Toftgard, 2000; Yang et al., 2008). In addition, an extended duration of GCP localization in the EGL might

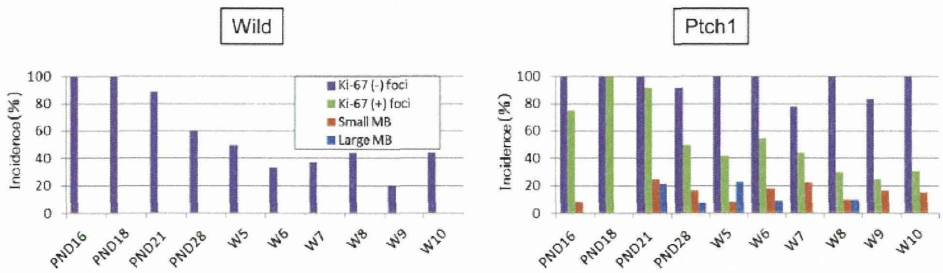

Fig. 9. Incidences of Ki-67-negative (−) and positive (+) foci and MBs in wild-type and Ptch1 mice. Incidences (%) were calculated as follows; number of animals which have specific lesion (e.g. Ki-67-negative foci) in the cerebellum relative to the total number of animals examined. Ki-67-negative foci were observed in both genotypes, but in higher incidence in Ptch1 mice throughout the examination period. Ki-67-positive foci had a tendency to decrease with aging. Small MB and large MB had no tendency to increase with aging.

Please cite this article in press as: Matsuo S, et al. Thickened area of external granular layer and Ki-67 positive focus are early events of medulloblastoma in *Ptch1*$^{+/-}$ mice. Exp Toxicol Pathol (2012), http://dx.doi.org/10.1016/j.etp.2012.12.005

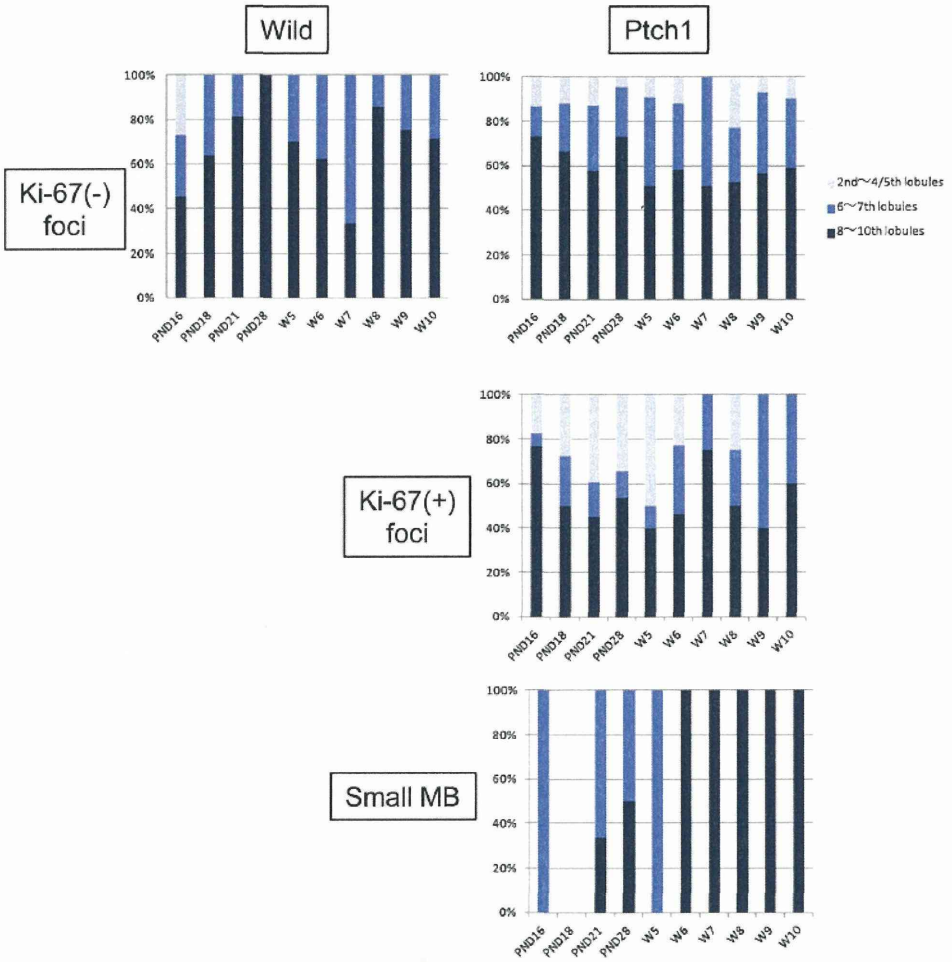

Fig. 10. Location of Ki-67-negative (−) and positive (+) foci and small MBs in the cerebellum of wild-type and Ptch1 mice. Incidences (%) were calculated as follows: total number of specific lesion per cerebellar lobule of all animal examined relative to total number of the lesion in the whole cerebellum of all animals examined.

increase opportunities for additional mutations which may lead to tumorigenesis (Corcoran and Scott, 2001; Wetmore et al., 2000).

Proliferative lesions such as preneoplastic lesions of MBs during 3 weeks after birth in Ptch1 mice were described as rare occurrences in previous reports (Kim et al., 2003); however, our detailed and sequential examination revealed that proliferative lesions and MBs had already been detected in Ptch1 mice within 3 weeks after birth. The morphology and immunohistochemistry of MBs at PND12 indicated that MBs arose from GCPs of the outer layer of the EGL during cerebellar development. The cells of the earliest proliferative lesion, focal thickened area of the EGL, showed the same immunohistochemical profiles as GCPs of the outer layer of the EGL. As the thickened area had cellular atypia and disarrangement compared to normal GCPs, it was considered to be preneoplastic of MB. The appearance of focal thickened proliferative lesions was limited during PND10 to PND14 when the EGL was detectable in this study. It may be that those lesions were recognized as Ki-67-positive foci or small MBs after PND16 because normal GCPs neighboring the lesions disappeared due to migration into the IGL after PND16.

We also found another preneoplastic lesion of MB derived from residual GCPs as Ki-67-positive focus only in Ptch1 mice. In previous reports, MBs were thought to arise from residual GCPs located at the surface of the cerebellum (Corcoran and Scott, 2001; Goodrich et al., 1997). In our study, the foci of GCP-like cells were found on the surface of the cerebellar cortex and only detectable on and after PND16. They were clearly divided into two types by the morphological and immunohistochemical profiles and genotypes. Observation of the EGL in BrdU-treated animal revealed that both types of the foci with BrdU-positive cells were composed of residual GCPs. The cells of Ki-67 positive foci had the same profiles as granular cells of the outer

Please cite this article in press as: Matsuo S, et al. Thickened area of external granular layer and Ki-67 positive focus are early events of medulloblastoma in *Ptch1*$^{+/-}$ mice. Exp Toxicol Pathol (2012), http://dx.doi.org/10.1016/j.etp.2012.12.005

layer of the EGL, indicating that they were undifferentiated and had high proliferating potential. The other focus, Ki-67-negative type, was composed of cells showing neuronal differentiation with a lack of proliferating activity. They resembled granular cells of the IGL or the inner layer of the EGL indicating that the cells were already differentiated into mature granular cells. The Ki-67-negative foci were detected in both genotypes. In addition, more than half of the Ki-67-positive foci were located in the 5–10th lobules of the cerebellum as well as in small MBs in Ptch1 mice. Although MBs are thought to be derived from residual GCPs located in the EGL of the cerebellum (Behesti and Marino, 2009; Roussel and Hatten, 2011), these results strongly suggest that residual GCPs in the Ki-67-positive foci were preneoplastic lesions. A high yield of Ki-67-positive foci may be useful as an easily detectable and confidential indicator of MB. These preneoplastic lesions might be useful as early markers to detect modulation effects of chemicals to shorten experimental periods.

The observation of a higher incidence of Ki-67-negative residual foci in Ptch1 mice as compared to wild-type mice and a reduced incidence of Ki-67-negative residual foci with increased age in wild-type mice was unexpected. These findings may be attributable to smaller Ki-67-negative foci in wild-type mice and a much lower number per animal as compared to Ptch1 mice, although their incidences were 100%. Chances to find the foci in a cross section of the cerebellum may have been reduced with increased age in wild-type mice due to cerebellar growth.

Purkinje cells secrete the mitogen Shh for GCP proliferation in the EGL during early phases of cerebellar development (Roussel and Hatten, 2011). After the GCPs lost cell proliferating activity, they migrate along radial fibers of Bergmann glia (Roussel and Hatten, 2011). It has been reported that abnormal development of Purkinje cells and Bergmann glia can disrupt proliferation, migration, and differentiation of GCPs (Adams et al., 2002; D'Arca et al., 2010; Rakic and Sidman, 1973; Schwartz et al., 1997). Our immunohistochemical results demonstrate no abnormal morphology in Bergmann glia or Purkinje cells, indicating that the MB formation process during cerebellar development might be intrinsic to the GCPs rather than abnormalities in Bergmann glia and Purkinje cells.

In conclusion, a thickened area of the EGL and Ki-67-positive foci were considered to be the early preneoplastic lesions of MBs derived from GCPs in the EGL in Ptch1 mice. These were distinguishable by immunohistochemistry with proliferation and neuronal differentiation markers. Preneoplastic lesions of MBs may serve as useful indicators and as substitutions for advanced MBs in the evaluation of drug efficacy and modulating effects of additional gene mutations, chemicals, and irradiation. Importantly, the Ki-67-positive focus is an easily detectable and confidential indicator due to higher occurrences in the third week after birth.

Acknowledgements

We thank Tomomi Morikawa for technical assistance in conducting the study and genotyping, and Miss Ayako Kaneko for technical assistance in histopathological preparation. This study was partly supported by Health and Labor Sciences Research Grants, Research on Risk of Chemical Substances, Ministry of Health, Labor and Welfare (H22-Toxicol-003).

References

Adams NC, Tomoda T, Cooper M, Dietz G, Hatten ME. Mice that lack astrotactin have slowed neuronal migration. Development 2002;129:965–72.
Aref D, Moffatt CJ, Agnihotri S, Ramaswamy V, Dubuc AM, Northcott PA, et al. Canonical TGF-beta pathway activity is a predictor of SHH-driven medulloblastoma survival and delineates putative precursors in cerebellar development. Brain Pathology 2012.
Ayrault O, Zindy F, Rehg J, Sherr CJ, Roussel MF. Two tumor suppressors, p27Kip1 and patched-1, collaborate to prevent medulloblastoma. Molecular Cancer Research 2009;7:33–40.
Behesti H, Marino S. Cerebellar granule cells: insights into proliferation, differentiation, and role in medulloblastoma pathogenesis. International Journal of Biochemistry and Cell Biology 2009;41:435–45.
Bhatia B, Potts CR, Guldal C, Choi S, Korshunov A, Pfister S, et al. Hedgehog-mediated regulation of PPARγ controls metabolic patterns in neural precursors and shh-driven medulloblastoma. Acta Neuropathologica 2012;123:587–600.
Briggs KJ, Corcoran-Schwartz IM, Zhang W, Harcke T, Devereux WL, Baylin SB, et al. Cooperation between the Hic1 and Ptch1 tumor suppressors in medulloblastoma. Genes and Development 2008;22:770–85.
Corcoran RB, Scott MP. A mouse model for medulloblastoma and basal cell nevus syndrome. Journal of Neuro-Oncology 2001;53:307–18.
Crawford JR, MacDonald TJ, Packer RJ. Medulloblastoma in childhood: new biological advances. The Lancet Neurology 2007;6:1073–85.
D'Arca D, Zhao X, Xu W, Ramirez-Martinez NC, Iavarone A, Lasorella A. Huwe1 ubiquitin ligase is essential to synchronize neuronal and glial differentiation in the developing cerebellum. Proceedings of the National Academy of Sciences of the United States of America 2010;107:5875–80.
Ellison DW, Dalton J, Kocak M, Nicholson SL, Fraga C, Neale G, et al. Medulloblastoma: clinicopathological correlates of SHH WNT, and non-SHH/WNT molecular subgroups. Acta Neuropathologica 2011;121:381–96.
Farioli-Vecchioli S, Tanori M, Micheli L, Mancuso M, Leonardi L, Saran A, et al. Inhibition of medulloblastoma tumorigenesis by the antiproliferative and pro-differentiative gene PC3. FASEB Journal 2007;21:2215–25.
Gavino C, Richard S. Patched1 haploinsufficiency impairs ependymal cilia function of the quaking viable mice, leading to fatal hydrocephalus. Molecular and Cellular Neurosciences 2011;47:100–7.
Goodrich LV, Milenkovic L, Higgins KM, Scott MP. Altered neural cell fates and medulloblastoma in mouse patched mutants. Science 1997;277:1109–13.
Gupta S, Takebe N, Lorusso P. Targeting the Hedgehog pathway in cancer. Therapeutic Advances in Medical Oncology 2010;2:237–50.
Hahn H, Wojnowski L, Miller G, Zimmer A. The patched signaling pathway in tumorigenesis and development: lessons from animal models. Journal of Molecular Medicine (Berlin, Germany) 1999;77:459–68.
Haldipur P, Bharti U, Govindan S, Sarkar C, Iyengar S, Gressens P, et al. Expression of Sonic hedgehog during cell proliferation in the human cerebellum. Stem Cells and Development 2012;21:1059–68.
Hatten ME, Roussel MF. Development and cancer of the cerebellum. Trends in Neurosciences 2011;34:134–42.
Huse JT, Holland EC. Targeting brain cancer: advances in the molecular pathology of malignant glioma and medulloblastoma. Nature Reviews Cancer 2010;10:319–31.
Jones DT, Jager N, Kool M, Zichner T, Hutter B, Sultan M, et al. Dissecting the genomic complexity underlying medulloblastoma. Nature 2012;488:100–5.
Kim JY, Nelson AL, Algon SA, Graves O, Sturla LM, Goumnerova LC, et al. Medulloblastoma tumorigenesis diverges from cerebellar granule cell differentiation in patched heterozygous mice. Developmental Biology 2003;263:50–66.
Kimura H, Stephen D, Joyner A, Curran T. Gli1 is important for medulloblastoma formation in Ptc1$^{+/-}$ mice. Oncogene 2005;24:4026–36.
Klesse LJ, Bowers DC. Childhood medulloblastoma: current status of biology and treatment. CNS Drugs 2010;24:285–301.
Kool M, Korshunov A, Remke M, Jones DT, Schlanstein M, Northcott PA, et al. Molecular subgroups of medulloblastoma: an international meta-analysis of transcriptome, genetic aberrations, and clinical data of WNT, SHH, Group 3, and Group 4 medulloblastomas. Acta Neuropathologica 2012;123:473–84.
Lau J, Schmidt C, Markant SL, Taylor MD, Wechsler-Reya RJ, Weiss WA. Matching mice to malignancy: molecular subgroups and models of medulloblastoma. Childs Nervous System 2012;28:521–32.
Mohan AL, Friedman MD, Ormond DR, Tobias M, Murali R, Jhanwar-Uniyal M. PI3K/mTOR signaling pathways in medulloblastoma. Anticancer Research 2012;32:3141–6.
Northcott PA, Korshunov A, Witt H, Hielscher T, Eberhart CG, Mack S, et al. Medulloblastoma comprises four distinct molecular variants. Journal of Clinical Oncology 2011;29:1408–14.
Oliver TG, Read TA, Kessler JD, Mehmeti A, Wells JF, Huynh TT, et al. Loss of patched and disruption of granule cell development in a pre-neoplastic stage of medulloblastoma. Development 2005;132:2425–39.
Pazzaglia S. Ptc1 heterozygous knockout mice as a model of multi-organ tumorigenesis. Cancer Letters 2006;234:124–34.
Pazzaglia S, Pasquali E, Tanori M, Mancuso M, Leonardi S, di Majo V, et al. Physical, heritable and age-related factors as modifiers of radiation cancer risk in patched heterozygous mice. International Journal of Radiation Oncology, Biology, Physics 2009;73:1203–10.
Pazzaglia S, Tanori M, Mancuso M, Gessi M, Pasquali E, Leonardi S, et al. Two-hit model for progression of medulloblastoma preneoplasia in Patched heterozygous mice. Oncogene 2006;25:5575–80.
Pogoriler J, Millen K, Utset M, Du W. Loss of cyclin D1 impairs cerebellar development and suppresses medulloblastoma formation. Development 2006;133:3929–37.
Raffel C. Medulloblastoma: molecular genetics and animal models. Neoplasia 2004;6:310–22.
Rakic P, Sidman RL. Weaver mutant mouse cerebellum: defective neuronal migration secondary to abnormality of Bergmann glia. Proceedings of the National Academy of Sciences of the United States of America 1973;70:240–4.

Please cite this article in press as: Matsuo S, et al. Thickened area of external granular layer and Ki-67 positive focus are early events of medulloblastoma in *Ptch1*$^{+/-}$ mice. Exp Toxicol Pathol (2012), http://dx.doi.org/10.1016/j.etp.2012.12.005

Roussel MF, Hatten ME. Cerebellum development and medulloblastoma. Current Topics in Developmental Biology 2011;94:235–82.
Schwartz PM, Borghesani PR, Levy RL, Pomeroy SL, Segal RA. Abnormal cerebellar development and foliation in BDNF −/− mice reveals a role for neurotrophins in CNS patterning. Neuron 1997;19:269–81.
Svärd J, Rozell B, Toftgard R, Teglund S. Tumor suppressor gene co-operativity in compound Patched1 and suppressor of fused heterozygous mutant mice. Molecular Carcinogenesis 2009;48:408–19.
Takahashi M, Matsuo S, Inoue K, Tamura K, Irie K, Kodama Y, et al. Development of an early induction model of medulloblastoma in Ptch1 heterozygous mice initiated with N-ethyl-N-nitrosourea. Cancer Science 2012.
Thomas WD, Chen J, Gao YR, Cheung B, Koach J, Sekyere E, et al. Patched1 deletion increases N-Myc protein stability as a mechanism of medulloblastoma initiation and progression. Oncogene 2009;28:1605–15.
Toftgard R. Hedgehog signalling in cancer. Cellular and Molecular Life Sciences 2000;57:1720–31.
Uziel T, Zindy F, Xie S, Lee Y, Forget A, Magdaleno S, et al. The tumor suppressors Ink4c and p53 collaborate independently with Patched to suppress medulloblastoma formation. Genes and Development 2005;19:2656–67.
Wang X, Venugopal C, Manoranjan B, McFarlane N, O'Farrell E, Nolte S, et al. Sonic hedgehog regulates Bmi1 in human medulloblastoma brain tumor-initiating cells. Oncogene 2012;31:187–99.
Wetmore C, Eberhart DE, Curran T. The normal patched allele is expressed in medulloblastomas from mice with heterozygous germ-line mutation of patched. Cancer Research 2000;60:2239–46.
Wetmore C, Eberhart DE, Curran T. Loss of p53 but not ARF accelerates medulloblastoma in mice heterozygous for patched. Cancer Research 2001;61:513–6.
Wu X, Northcott PA, Croul S, Taylor MD. Mouse models of medulloblastoma. Chinese Journal of Cancer 2011;30:442–9.
Yang ZJ, Ellis T, Markant SL, Read TA, Kessler JD, Bourboulas M, et al. Medulloblastoma can be initiated by deletion of Patched in lineage-restricted progenitors or stem cells. Cancer Cell 2008;14:135–45.

Please cite this article in press as: Matsuo S, et al. Thickened area of external granular layer and Ki-67 positive focus are early events of medulloblastoma in *Ptch1*$^{+/-}$ mice. Exp Toxicol Pathol (2012), http://dx.doi.org/10.1016/j.etp.2012.12.005